Microbial biogeography of wine grapes is conditioned by cultivar, vintage, and climate

Nicholas A. Bokulich[a,b,c], John H. Thorngate[d], Paul M. Richardson[e], and David A. Mills[a,b,c,1]

Departments of [a]Viticulture and Enology and [b]Food Science and Technology, and [c]Foods for Health Institute, University of California, Davis, CA 95616; [d]Constellation Brands, Inc., Saint Helena, CA 94574; and [e]MicroTrek, Inc., San Francisco, CA 94104

Edited by Robert Haselkorn, University of Chicago, Chicago, IL, and approved October 25, 2013 (received for review September 16, 2013)

Wine grapes present a unique biogeography model, wherein microbial biodiversity patterns across viticultural zones not only answer questions of dispersal and community maintenance, they are also an inherent component of the quality, consumer acceptance, and economic appreciation of a culturally important food product. On their journey from the vineyard to the wine bottle, grapes are transformed to wine through microbial activity, with indisputable consequences for wine quality parameters. Wine grapes harbor a wide range of microbes originating from the surrounding environment, many of which are recognized for their role in grapevine health and wine quality. However, determinants of regional wine characteristics have not been identified, but are frequently assumed to stem from viticultural or geological factors alone. This study used a high-throughput, short-amplicon sequencing approach to demonstrate that regional, site-specific, and grape-variety factors shape the fungal and bacterial consortia inhabiting wine-grape surfaces. Furthermore, these microbial assemblages are correlated to specific climatic features, suggesting a link between vineyard environmental conditions and microbial inhabitation patterns. Taken together, these factors shape the unique microbial inputs to regional wine fermentations, posing the existence of nonrandom "microbial *terroir*" as a determining factor in regional variation among wine grapes.

viticulture | agriculture | metagenomics | next-generation sequencing

Microbial biogeography, the study of microbial biodiversity over time and space (1), uncovers the role that geospatial dispersion patterns play in human health (2), environmental inhabitation (3), indoor environments (4), and agriculture (5), revealing important links between environmental conditions, microbial communities, and macroscopic phenomena. *Vitis vinifera* (wine grape) represents an economically and culturally important agricultural crop for which microbial activity plays critical roles in grape (6) and wine production and quality formation (7, 8). Indeed, regional variation in grape- and wine-quality characteristics is a critical feature of perceived product identity (*terroir*), with significant consequences for consumer preference and economic appreciation (9). However, scant evidence exists for nonrandom microbial distribution patterns in grapes and wines (6, 10) and the factors driving microbial assemblages on grape surfaces are unknown. Given that many of the same environmental conditions that govern regional variations in grapevine growth and development (11) also alter microbial communities across space and time (1), it follows that biogeographical assemblages of grape-surface microbiota may exist, potentially influencing grapevine health and wine quality.

The *V. vinifera* phyllosphere is colonized by bacteria and fungi that substantially modulate grapevine health, development, and grape and wine qualities (6). Many microbes inhabiting the grape surface cannot survive the low-pH, ethanolic, anaerobic conditions of wine fermentations, but their metabolic activity on the grape surface can have long-ranging consequences, such as the metabolic changes wrought by phytopathogenic fungi (12, 13). However, some grape-surface microbes can grow and survive in wine fermentations (14), and several are implicated in wine spoilage downstream (7). This is particularly true of grapes damaged by disease or pest pressure, which have been shown to contain elevated populations of bacteria such as *Acetobacteraceae* and yeasts such as *Zygosaccharomyces* (15, 16). The impact of grape microbiota is often beneficial, and the participation of indigenous microbiota in wine fermentations is often considered to enhance the sensory complexity of wines (17). Bioprospecting the microbiota of wine fermentations has led to the discovery of several species with positive enological properties, which are now commercially available as coinocula with *Saccharomyces* yeasts in winemaking (17). Consequently, a growing number of yeasts and bacteria are being recognized as active participants in wine fermentations with important contributions to wine sensory qualities (17).

Nevertheless, whether grape-surface microbiota are nonrandomly distributed in the environment is disputed (6), and little work has been done to test the impact of natural factors, such as climate, growing region, and cultivar on grape microbiota. Geographical delineations among *Saccharomyces cerevisiae* populations and cultivable yeast communities in New Zealand vineyards have been documented previously, providing evidence for regional dispersion of vineyard yeasts (18). However, it is unknown whether nonrandom geographical dispersion patterns exist among the complete grape-surface microbiota and how these communities are formed, explaining relationships between environmental growing conditions and the microbial consortium living on and interacting with wine grapes. Historically, microbial surveillance efforts have been limited by the throughput and methodological biases of culture-based techniques and low resolution of early molecular ecology techniques (19, 20). However, recent advances in massively parallel, short-amplicon sequencing technologies have launched

Significance

We demonstrate that grape-associated microbial biogeography is nonrandomly associated with regional, varietal, and climatic factors across multiscale viticultural zones. This poses a paradigm shift in our understanding of food and agricultural systems beyond grape and wine production, wherein patterning of whole microbial communities associated with agricultural products may associate with downstream quality characteristics. Elucidating the relationship between production region, climate, and microbial patterns may enhance biological control within these systems, improving the supply, consumer acceptance, and economic value of important agricultural commodities.

Author contributions: N.A.B., J.H.T., P.M.R., and D.A.M. designed research; N.A.B. performed research; D.A.M. contributed new reagents/analytic tools; N.A.B. analyzed data; and N.A.B., J.H.T., and D.A.M. wrote the paper.

Conflict of interest statement: N.A.B., P.M.R., and D.A.M. all own shares of MicroTrek, Inc. a service laboratory serving the food and beverage industry.

This article is a PNAS Direct Submission.

Freely available online through the PNAS open access option.

Data deposition: Raw data are publicly deposited in QIIME-db (www.microbio.me/qiime/) as studies 2019 (bacterial 16S rRNA sequences) and 2020 (fungal ITS sequences).

[1]To whom correspondence should be addressed. E-mail: damills@ucdavis.edu.

This article contains supporting information online at www.pnas.org/lookup/suppl/doi:10.1073/pnas.1317377110/-/DCSupplemental.

a breakthrough in microbial ecology studies of wine- and food-fermentation systems (14, 21–27), putting hitherto untenable ecological questions within reach.

Results and Discussion

Regional Origin Defines Grape Must Microbial Patterns. To elucidate connections between growing region, cultivar, climate, and microbial biogeography, 273 grape must samples were collected from across California in two separate vintages (*SI Appendix*, Fig. S1). Must consists of destemmed, crushed grapes, representing a mixed, aggregate sample of all grapes from an individual vineyard block. These samples were collected in the wineries immediately following crushing and mixing, frozen, and analyzed with a short-amplicon sequencing approach to characterize both fungal and bacterial community compositions. Fungal profiles were dominated by filamentous fungi, primarily *Cladosporium* spp. (28.2% average relative abundance), *Botryotinia fuckeliana* (*Botrytis cinerea*) (15.2%), *Penicillium* spp. (9.5%), *Davidiella tassiana* (9.2%), and *Aureobasidium pullulans* (7.3%), with notable populations of yeasts, including *S. cerevisiae* (4.0%), *Hanseniaspora uvarum* (5.0%), and *Candida zemplinina* (1.3%) (Dataset S1). Bacterial communities predominantly consisted of the orders *Lactobacillales* (29.7%), *Pseudomonadales* (14.2%), *Enterobacteriales* (13.5%), *Bacillales* (12.6%), and *Rhodospirillales* (5.1%) (Dataset S2). Community structure varied widely across different grape-growing regions, exerting a significant impact on both fungal taxonomic dissimilarity (Bray–Curtis $R_{ANOSIM} = 0.265$, $P < 0.001$; ANOSIM, analysis of similarities) and bacterial genetic diversity (weighted UniFrac $R_{ANOSIM} = 0.088$, $P < 0.001$) independent of other variables, including variety and vintage (*SI Appendix*, Fig. S2 and Table 1). These variables are apparently confounding factors, as clustering patterns become more distinct and regression coefficients improve when comparing regional differences within single grape varieties (Fig. 1, *SI Appendix*, Fig. S3, and Table 1) and within single years (Table 1).

The most commonly grown grape varieties in California, Chardonnay and Cabernet Sauvignon, were analyzed independently to dissect intravarietal biogeographical relationships. Chardonnay musts display highly significant regional patterns for fungal ($R_{ANOSIM} = 0.331$, $P < 0.001$) and bacterial communities ($R_{ANOSIM} = 0.249$, $P = 0.002$) across both vintages (Fig. 1 and Table 1). Cabernet Sauvignon exhibits significant regional patterns for fungal communities across both vintages ($R_{ANOSIM} = 0.339$, $P < 0.001$) but weak or no significance for bacterial communities across both vintages ($R_{ANOSIM} = 0.046$, $P = 0.189$; $R^2_{ADONIS} = 0.094$, $P = 0.002$; ADONIS, permutational multivariate analysis of variance) and for the 2010 vintage alone ($R_{ANOSIM} = 0.067$, $P = 0.051$; $R^2_{ADONIS} = 0.094$, $P = 0.014$) (*SI Appendix*, Fig. S3 and Table 1). Bacterial weighted UniFrac distance (28)—a measure of phylogenetic similarity between samples—reveals that must community similarities follow a geographical axis running roughly parallel to the California coastline ($P = 0.021$) (Fig. 1*A*), suggesting that environmental patterns may underlie these regional trends. Whereas fungal Bray–Curtis dissimilarity patterns exhibit clear differences between regions for both Chardonnay and Cabernet Sauvignon, only Cabernet Sauvignon musts are significantly associated with this coastal geographical axis ($P < 0.001$) (*SI Appendix*, Fig. S3*B*). Chardonnay musts cluster by region but do not follow any apparent geographical axis (*SI Appendix*, Fig. S3*B*). Canonical discriminant analysis (CDA) of the predominant bacterial and fungal taxa reveals regional taxonomic associations, which are frequently conserved across varieties and vintages (*SI Appendix*, Fig. S2 *C* and *D*) as well as within individual varieties (Fig. 1*C* and *SI Appendix*, Figs. S3*D* and S4). Least discriminant analysis (LDA) effect size confirms that many of these trends relate to significant associations between microbial phyla and viticultural areas, with *Firmicutes* and *Eurotiomycetes* (including *Aspergillus* and *Penicillium*) being more abundant in Napa Chardonnay musts; *Bacteroides*, *Actinobacteria*, *Saccharomycetes*, and *Erysiphe necator* in Central Coast; and *B. fuckeliana* and *Proteobacteria* in Sonoma (Fig. 1*D* and Datasets S3 and S4). In Cabernet Sauvignon musts, *Eurotiomycetes* (including *Aspergillus* and *Penicillium*), *Sordariomycetes*, *Lactobacillus*, and *Bacteroidetes* are associated with North San Joaquin Valley musts; *Leotiomycetes* (notably *B. fuckeliana* and *E. necator*) *C. zemplinina* with Central Coast; *Dothideales* (e.g., *A. pullulans*), *Agaricomycetes*, and *Lactobacillales* with Sonoma; and *Pichiaceae* and *D. tassiana* with Napa (*SI Appendix*, Fig. S3*C* and Datasets S5 and S6).

To further confirm the stability of these observations across different conditions, a Random Forest supervised-learning model was used to identify which taxa explain the strongest variation in growing regions. This method determines the diagnostic power of bacterial and fungal profiles for predicting regional origin by

Table 1. ANOSIM and permutational MANOVA of category effects on microbial diversity patterns

			Fungal Bray–Curtis				Bacterial weighted UniFrac			
			ANOSIM		ADONIS		ANOSIM		ADONIS	
Group	Vintage	Factor	R	*P*	R^2	*P*	R	*P*	R^2	*P*
All	All	Region	0.265	0.001	0.137	0.001	0.088	0.001	0.066	0.001
All	2010	Region	0.255	0.001	0.139	0.001	0.095	0.001	0.075	0.001
Cabernet	All	Region	0.339	0.001	0.244	0.001	0.046	0.189	0.094	0.002
Cabernet	2010	Region	0.432	0.001	0.280	0.001	0.067	0.051	0.094	0.014
Chardonnay	All	Region	0.331	0.001	0.229	0.001	0.249	0.002	0.205	0.001
Chardonnay	2010	Region	0.426	0.001	0.317	0.001	0.437	0.001	0.289	0.001
All	All	Variety	0.248	0.001	0.239	0.001	0.100	0.001	0.129	0.001
CHZ	All	Variety	0.364	0.001	0.201	0.001	0.060	0.015	0.042	0.001
CHZ	2010	Variety	0.370	0.001	0.219	0.001	0.047	0.022	0.036	0.002
Sonoma CHZ	2010	Variety	0.553	0.001	0.373	0.001	0.298	0.001	0.231	0.001
Napa ABCD	All	Vineyard	0.469	0.001	0.672	0.001	0.024	0.403	0.112	0.440
Napa ABCD	2012	Vineyard	0.442	0.001	0.425	0.001	0.142	0.188	0.284	0.174
All	All	Vintage	0.101	0.054	0.036	0.001	0.025	0.306	0.024	0.001
Napa ABCD	All	Vintage	0.044	0.320	0.123	0.008	0.346	0.001	0.126	0.001

CHZ, all Cabernet Sauvignon, Chardonnay, and Zinfandel samples; Napa ABCD, all Chardonnay musts from Napa vineyards A–D.

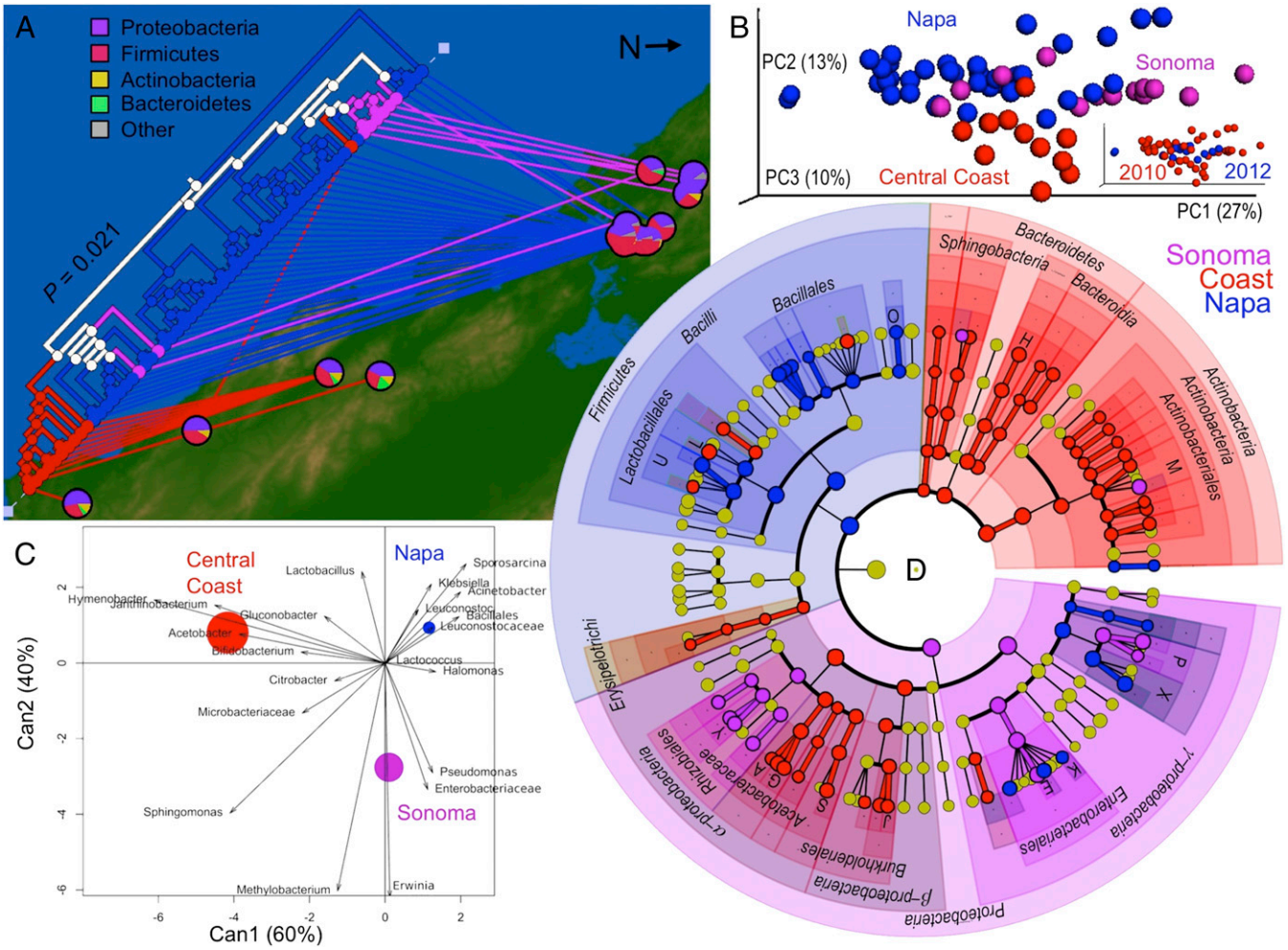

Fig. 1. Grape must bacterial communities demonstrate distinct regional patterns. (*A*) Weighted UniFrac distance dendrogram comparing bacterial communities of Chardonnay musts from across California. Branches are colored by the growing regions they represent, white branches encompass two or more regions. Pie charts represent average phylum-level taxonomic compositions of all samples from each site. *P* value represents goodness-of-fit scores between tree topology and sample ordination along the geographical axis. Map adapted from Oak Ridge National Lab Distributed Active Archive Center for Biogeochemical Dynamics spatial data access tool (http://webmap.ornl.gov/). (*B*) Weighted UniFrac distance PCoA of bacterial communities in Chardonnay musts from across California. (*Inset*) Same plot categorized by vintage. (*C*) Canonical discriminant analysis plot comparing Chardonnay musts from Napa, Sonoma, and Central Coast growing regions coplotted against bacterial taxa loadings. Circles represent canonical group means and 95% confidence interval for each class, which are significantly different if their confidence intervals do not overlap. Arrows represent the degree of correlation between each taxon and each class as a measure of predictive discrimination of each class. (*D*) LDA effect size taxonomic cladogram comparing all Chardonnay musts categorized by growing region. Significantly discriminant taxon nodes are colored and branch areas are shaded according to the highest-ranked variety for that taxon. For each taxon detected, the corresponding node in the taxonomic cladogram is colored according to the highest-ranked group for that taxon. If the taxon is not significantly differentially represented between sample groups, the corresponding node is colored yellow. Highly abundant and select taxa are indicated: A, *Acetobacter*; E, *Erwinia*; G, *Gluconobacter*; H, *Hymenobacter*; J, *Janthinobacterium*; K, *Klebsiella*; L, *Lactobacillus*; M, *Microbacteriaceae*; O, *Sporosarcina*; P, *Pseudomonadaceae;* S, *Sphingomonas*; U, *Leuconostocaceae*; X, *Moraxellaceae*; Y, *Methylobacterium*. For the complete list of discriminate taxa and ranks used to generate this cladogram, see Dataset S4.

using a subset of samples to train a model that identifies unique features within data categories. The technique then determines the accuracy of the model by categorizing sample subsets that were not used to build the model. Fungal models display a large degree of predictive power (observed error range 0.146–0.188; ratio to random error 2.449–4.592), particularly when all must samples are included regardless of variety or vintage (error 0.146 ± 0.055; ratio 4.592) (*SI Appendix*, Table S1). Bacterial models for all must samples (error 0.282 ± 0.076; ratio 2.325) and Chardonnay must samples (error 0.085 ± 0.116; ratio 4.914) perform well, but vintage-controlled and Cabernet Sauvignon models yield high error rates (*SI Appendix*, Table S1). The most important taxonomic features for regional prediction in these models are many of the same significant taxa identified by CDA and LDA, including *Pseudomonas*, *Acetobacter*, and *Cladosporium* spp. (*SI Appendix*, Table S2).

These results reveal that nonrandom regional distributions of grape microbiota exist across large geographical scales. Growing regions can be distinguished based on the abundance of several key fungal and bacterial taxa, defining potentially predictive regional features with obvious consequences for grapevine management and wine quality. The chemicosensory distinction of wines from different growing regions is well established (29–33), providing the conceptual basis of wine *terroir*, although the causative factors are elusive (9). Likewise, the formative influences of many key grape-derived microbiota on wine quality

characteristics are well described (6–8, 17, 34), but whether their geographical distribution follows logical patterns—supporting a causative role in regional wine differences—has been unknown (6). Thus, the nonrandom distribution of key taxa with crucial impacts on wine quality supports the potential role of microbial biogeography in shaping wine *terroir*. Many of the taxonomic discriminants identified between growing regions are organisms that can participate in wine fermentations. Most *Saccharomycetes*, including *S. cerevisiae*, the primary driver of wine fermentations, are notably nondiscriminant (*SI Appendix*, Fig. S3). However, important exceptions exist, including *C. zemplinina*, *Lachancea thermotolerans*, *Hanseniaspora guilliermondii*, and *Pichia* spp., fermentative yeasts with known chemicosensory impacts in wine fermentations (17, 34). Additionally, discriminant populations of *Acetobacteraceae* and *Lactobacillales* represent sources of additional quality variation, being important organisms in wine spoilage (7, 8, 16) and the latter in malolactic wine fermentations (7, 8). These connections provide compelling support for the role of grape-surface microbial communities in regional wine characteristics. Differences in these fermentative populations can conceivably underlie regional patterns in fermentation performance and product qualities, participating in the formation of *terroir*-associated wine characteristics. Whether these patterns actively drive quantifiably discriminate chemicosensory characteristics must be experimentally demonstrated to fully establish microbial *terroir* as a determining feature of wine qualities, but these results nevertheless provide a compelling basis to explore these relationships on macroregional scales.

Grape Variety Influences Grape Must Microbiota. Grape variety also plays a significant role in shaping microbial community patterns across all regions and vintages (fungal Bray–Curtis R_{ANOSIM} = 0.248, $P < 0.001$; bacterial weighted UniFrac R_{ANOSIM} = 0.100, $P < 0.001$) (Table 1 and *SI Appendix*, Fig. S5). Fungal community differences are apparent among the most highly sampled varieties (Cabernet Sauvignon, Chardonnay, and Zinfandel) (R_{ANOSIM} = 0.364, $P < 0.001$) (Table 1 and Fig. 2) but bacterial communities exhibit weak separations among these varieties compared across all growing regions (R_{ANOSIM} = 0.060, P = 0.015) (Table 1). For both fungal (R_{ANOSIM} = 0.553, $P < 0.001$) and bacterial communities (R_{ANOSIM} = 0.298, $P < 0.001$), varietal variation is most powerful within individual regions (Table 1 and Fig. 2). These varietal–microbial patterns appear highly stable year to year and controlling for vintage yields little improvement in regression coefficients (Table 1) and does not appear to confute clustering patterns (Fig. 2). However, bacterial communities appear strongly influenced by region, and controlling for regional variation greatly improves regression coefficients (Table 1) and clustering patterns (Fig. 2). CDA, LDA, and ANOVA demonstrate broad taxonomic trends underlying varietal patterns, with *Proteobacteria*, *Capnodiales* (including *Cladosporium* spp.), and *Penicillium* significantly more abundant in Chardonnay; *β-Proteobacteria*, *Bacteroidetes*, *Clostridia*, *Dothideomycetes*, *Agaricomycetes*, *Tremellomycetes*, *Microbotryomycetes*, and *Saccharomycetaceae* in Cabernet Sauvignon; and *Firmicutes*, *Gluconobacter*, *Eurotiomycetes* (*Aspergillus*), *Leotiomycetes*, and *Saccharomycetes* (notably *C. zemplinina*) in Zinfandel (Fig. 2, *SI Appendix*, Fig. S5, and Datasets S7 and S8).

Varietal patterns in grape-surface microbiota suggest a genetic component to host–microbial interactions on the grape surface. Relationships between grape variety and the abundance of yeast (35, 36) and bacterial species (37) on berry surfaces have been documented previously on very limited scales, but not statistically demonstrated. Cultivar differences in growth habit and stress and invasion response (38) could explain how *Vitis* manages (or incurs) its grape-surface microbial ecosystems, explaining both the "normal" microbiota and cultivar-specific susceptibilities to disease pressures under different environments. Many of the observed patterns support this hypothesis. For example, the thin skins and dense growth habit of Zinfandel fruit result in overcrowding and berry breakage (39). This effect likely explains the elevated abundances of *Gluconobacter*, *Lactobacillales*, and fermentative yeasts (notably *C. zemplinina*) on the surface of Zinfandel grapes (Fig. 2), as these organisms are enriched on damaged fruit (6, 15, 40). However, unlike biogeographical patterns, nonrandom microbial patterns linked to grape variety may also represent the influence of viticultural practices. Many cultivars receive specific treatments, including trellising and canopy management strategies, which alter grape microclimate, composition (41, 42), and hence possibly microbial community patterns.

No matter the underlying mechanism, the formation of robust cultivar-specific microbial patterns raises several opportunities for wine-quality management. Many of the variety-discriminant taxa are fermentative organisms, and may play a role in determining positive or negative chemicosensory features of ensuing wine fermentations (8). For example, undesired acetate production by *Gluconobacter* (16), malate conversion, off-flavor production by lactic acid bacteria (7, 8), or desirable enhancement of the sensory profile by *C. zemplinina* (43) all represent wine-quality impacts imparted by the cultivar-discriminative taxa detected in this study. Given the demonstrable relationship between these taxa and specific grape varieties, customized fermentation management strategies could improve product outcomes, e.g., through moderating sulfite additions, temperature control, oxygen limitation, inoculation, or cold maceration (to name only a few treatments) to promote or suppress individual populations based on the modeled microbial composition of a given grape variety. For example, significant associations between Zinfandel and *Gluconobacter* warrant extra attention to sulfite additions and oxygen exposure to prevent excess volatile acidity production in fermentations with this variety.

Environmental Conditions Modify Grape Microbiota Across Space and Time. Regional patterns in grape must microbiota suggest that local environmental conditions are responsible for driving biogeographical diversity. A high degree of correlation exists between different climatic and topographical features (*SI Appendix*, Fig. S6), and all environmental metrics display significant differences between regions (*SI Appendix*, Table S3). A best variables rank correlation test (BEST) was used to determine which of these factors explain the greatest degree of microbial community β-diversity dissimilarity, followed by permutational MANOVA tests to confirm significance. BEST identified average evapotranspiration (ET_0), net wind run, minimum temperature, and relative humidity (RH) as prevailing features for multiple sample subsets (*SI Appendix*, Table S4), with latitude, longitude, minimum temperature, average high temperature, average temperature, and average soil temperature all ranking highly. MANOVA determined that all features are highly significantly ($P < 0.05$) related to fungal and bacterial patterns in all must samples, with the exception of soil temperature in bacterial communities, and most features are significant ($P < 0.05$) among Chardonnay and Cabernet Sauvignon must samples (*SI Appendix*, Table S5). However, many features identified by BEST yield poor MANOVA R^2 coefficients, suggesting weakly significant feature importance (*SI Appendix*, Table S5). MANOVA identifies net precipitation, maximum temperature, RH, latitude, and longitude as the strongest features explaining microbial community dissimilarities across most subcategories, particularly for fungal community patterns (*SI Appendix*, Table S5). Significant covariance between each of these factors ($P < 0.05$) (*SI Appendix*, Fig. S6) complicates identification of potentially causative features, but weak MANOVA R^2 coefficients (explaining less variance than region alone) imply multiple interacting factors are responsible for the complex process of regional conditioning.

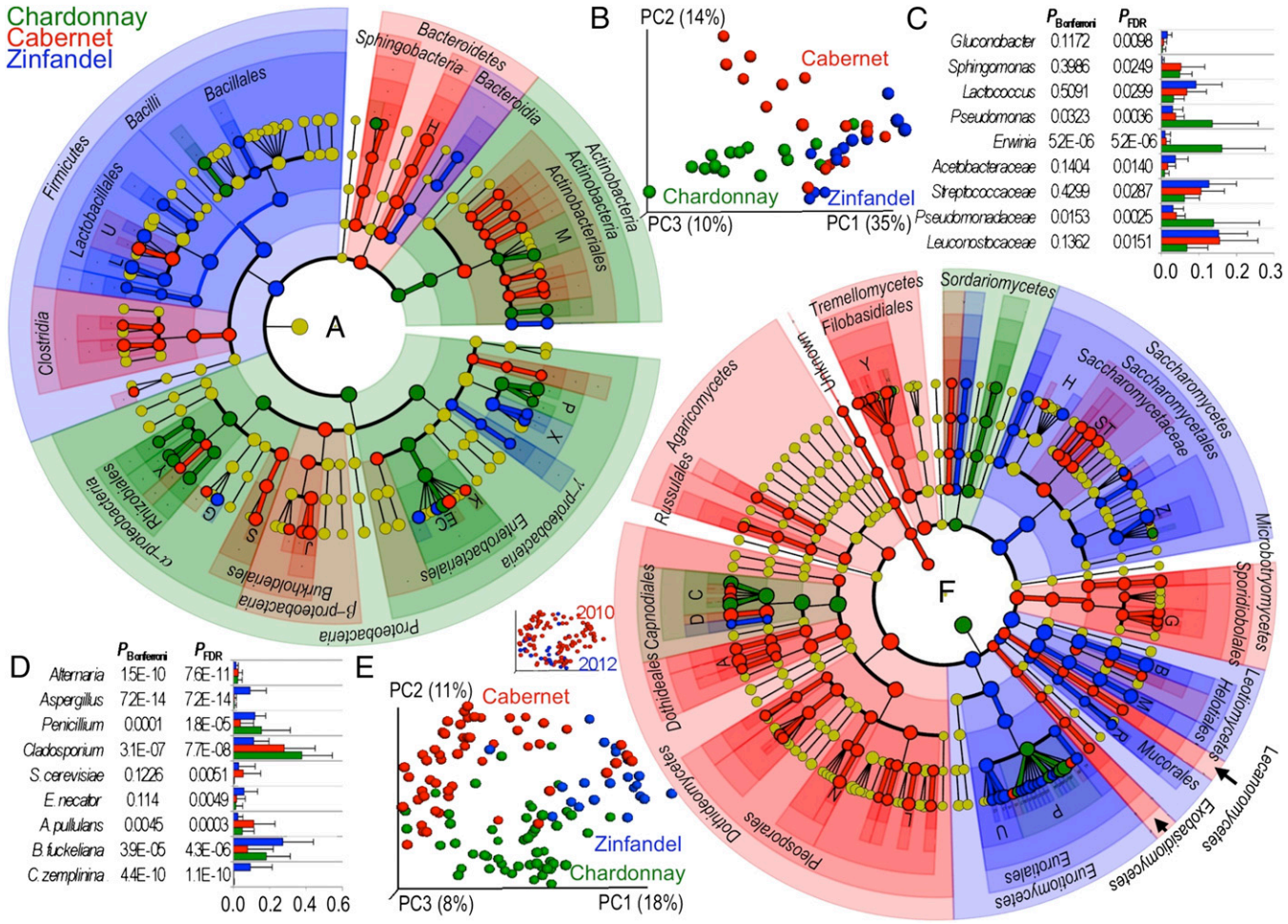

Fig. 2. Varietal variation in bacterial (*Left*) and fungal (*Right*) communities of Zinfandel, Cabernet Sauvignon, and Chardonnay grape musts. (*A*) LDA effect size taxonomic cladogram comparing bacterial communities in all Sonoma Cabernet Sauvignon, Chardonnay, and Zinfandel musts. Significantly discriminant taxon nodes are colored and branch areas are shaded according to the highest-ranked variety for that taxon. For each taxon detected, the corresponding node in the taxonomic cladogram is colored according to the highest-ranked group for that taxon. If the taxon is not significantly differentially represented between sample groups, the corresponding node is colored yellow. Highly abundant and select taxa are indicated: C, *Citrobacter*; E, *Erwinia*; G, *Gluconobacter*; H, *Hymenobacter*; J, *Janthinobacterium*; K, *Klebsiella*; L, *Lactococcus*; M, *Microbacteriaceae*; P, *Pseudomonadaceae*; S, *Sphingomonas*; U, *Leuconostocaceae*; X, *Moraxellaceae*; Y, *Methylobacterium*. (*B*) Weighted UniFrac distance PCoA of bacterial communities in all Sonoma Cabernet Sauvignon, Chardonnay, and Zinfandel musts. (*C* and *D*) One-way ANOVA of select bacterial (*C*) and fungal taxa (*D*) exhibiting significant differences between grape varieties. The *x* axes represent relative abundance (maximum 1.0). Bonferroni-corrected and false-discovery-rate (FDR) corrected *P* values are shown. (*E*) Bray–Curtis dissimilarity PCoA of fungal communities in all Cabernet Sauvignon, Chardonnay, and Zinfandel musts. (*Inset*) Same plot categorized by vintage. The *x* axis represents relative abundance (maximum 1.0). (*F*) LDA effect size taxonomic cladogram comparing fungal communities in all Cabernet Sauvignon, Chardonnay, and Zinfandel musts in all regions. Significantly discriminant taxon nodes are colored and branch areas are shaded according to the highest-ranked variety for that taxon. Highly abundant and select taxa are indicated: A, *Aureobasidium pullulans*; B, *Botryotinia fuckeliana*; C, *Cladosporium; D,* Davidiella; G, *Rhodotorula glutinis*; H, *Hanseniaspora*; M, *Erysiphe necator*; N, *Sclerostagonospora opuntiae*; P, *Penicillium*; R, *Rhizopus oryzae*; S, *Saccharomyces cerevisiae*; T, *Lachancea thermotolerans;* U, *Aspergillus*; Y, *Cryptococcus*; Z, *Candida zemplinina*. For the complete list of discriminate taxa and ranks used to generate these cladograms, see Datasets S7 and S8.

To elucidate which of these climatic conditions may drive specific microbial populations across growing regions and vintages, partial least squares regression (PLSR) was used to model covariance between environmental features and bacterial and fungal taxa at multiple taxonomic levels. PLSR projections were initially made between all order- to species-level taxa detected (Fig. 3 and *SI Appendix*, Fig. S7) and used to select taxa explaining >30% of the variance in the first two components. Projections of these extracted features reveal highly covariable relationships between several climatic conditions and microbial taxa (Fig. 3 and *SI Appendix*, Fig. S7). Notably, net precipitation associates strongly with *Mycosphaerellaceae*, *B. fuckeliana*, and *Pseudomonadales*; RH with *Moraxellaceae* and *Cladosporium*; and maximum temperature and average low temperature associate negatively with *Penicillium*, *Pseudomonas*, *Enterobacteriaceae*, and *Leuconostocaceae* (*Oenococcus oeni*) in Chardonnay musts (Fig. 3). Scatterplots and correlation coefficients were generated between these variables and factors to test the strength of the PLSR model, confirming noisy but significant ($P < 0.05$) correlations for many of these observations (*SI Appendix*, Figs. S8 and S9).

The apparent modification of grape microbial consortia by environmental factors suggests that biogeographical trends are responsive to local conditions, as opposed to being shaped by physical patterns of microbial dispersion, a finding with powerful implications for the future of wine-grape cultivation. First, some of these conditions can be modified by viticultural practices, so trellising types, canopy management, and other methods may be selected to alter the microclimate of the fruiting zone in an at-

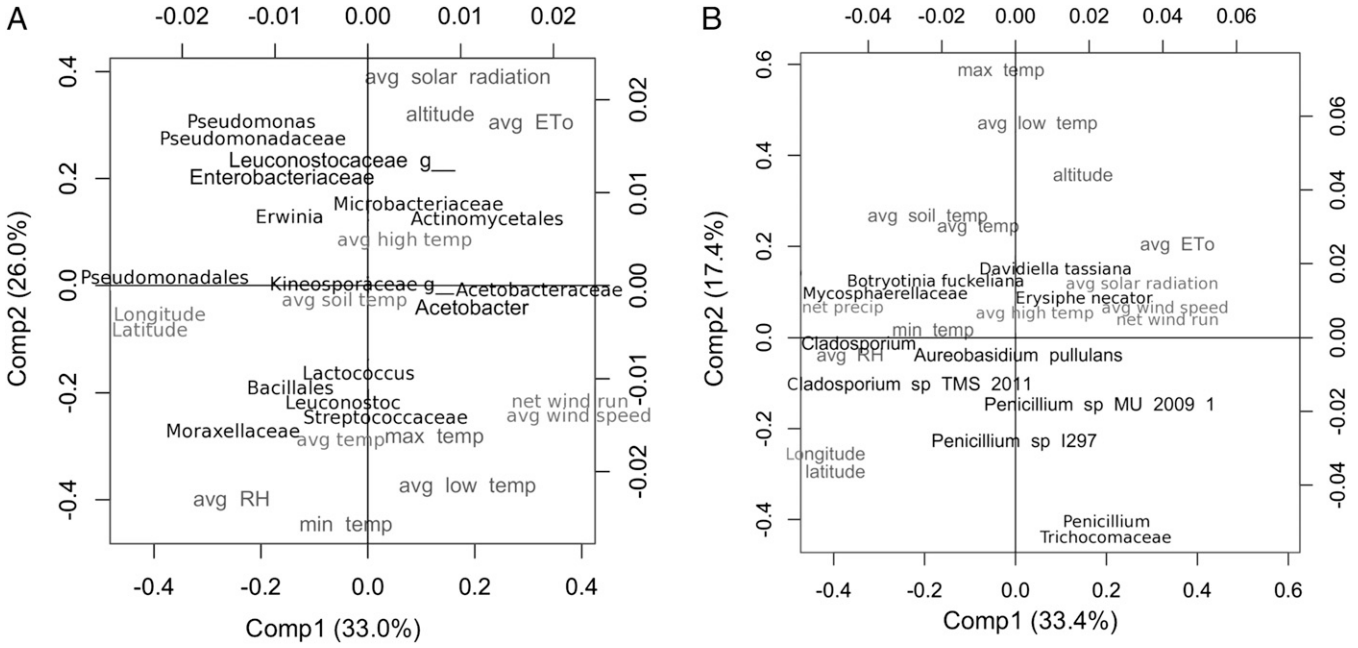

Fig. 3. Correlation loading plots demonstrate environmental influence on select microbial populations within Chardonnay musts across California. Partial least squares regression correlation loadings of 15 environmental variables (gray text) and select microbial taxa (black text). (*A*) Selected bacterial populations (n = 18 variables) of all Chardonnay musts. (*B*) Selected fungal populations (n = 12 variables) of all Chardonnay musts.

tempt to positively shape the microbial consortium. Such practices already see some employment, such as reducing canopy density to control mold growth (44). Second, the juggernaut of climate change threatens not only the sensitive geographic range and water availability for viticultural practices (45), but also the microbial ecologies of grape surfaces, potentially altering susceptibility to phytopathogen enrichment. The mounting risks of some phytopathogens under changing growing conditions have already been considered (46, 47) but the complete implications for the grape-surface microbiome is undefined. These findings present a platform from which to experimentally test these factors and whether microclimate modification procedures (e.g., trellising, shoot thinning, leaf removal) may be used to responsively manage grape-surface microbial communities.

These trends also permit development of predictive models for interpolation of microbial response across a greater geographical range and under variable climatic conditions. Such models could be useful in predicting microbial community responses under different combinations of grape variety and local conditions when selecting new vineyard sites or forecasting the impact of weather and climate change on grape microbial communities. Similar models are already used for the prediction of specific grapevine pathogen threats in response to environmental conditions (48–50) and to model large-scale biogeographical predictions (51). To be most effective outside of the established zones in this study, these observations need to be expanded to capture a greater variety of environmental conditions and global growing regions. Microbial dispersion limits may play a role in community assembly under global conditions (1) and must also be defined to avoid overfitting to Californian conditions. If regional factors define the "microbial *terroir*" of grape surfaces within this confined region, global viticultural zones may likewise express disparate microbial patterns and warrant further investigation.

Vintage Effects Exert Seasonal Shifts in Grape-Surface Microbiota Within Single Vineyards. Environmental effects exhibit temporal as well as spatial variation, yet vintage appears to have little effect on macroregional or varietal microbial patterns (Table 1). To elucidate the scale and impact of vintage on must microbial communities within microregions, four Chardonnay vineyards (vineyards A–D) in Napa Valley (all <4 km apart) were highly sampled in 2010 and 2012 to compare within and between vintages. Vintage has only a weak or insignificant impact on variation within all California must samples (Table 1). However, within these four vineyards alone bacterial communities see a significant vintage influence (R_{ANOSIM} = 0.346, P = 0.001), although fungal communities see a weak vintage effect (R_{ANOSIM} = 0.044, P = 0.320; R^2_{ADONIS} = 0.123, P = 0.008). Conversely, vineyard-specific patterns have a greater impact on fungal communities (R_{ANOSIM} = 0.469, P < 0.001) (Table 1 and Fig. 4). Thus, between-vintage variations substantially affect microbial communities within small geographical scales (i.e., individual vineyards), but not large scales (i.e., macroregions). CDA highlights the association between several key taxa and each vintage (Fig. 4). Notably, *Cladosporium* and *B. fuckeliana* are more abundant in 2010 samples, whereas *Penicillium*, *Pseudomonas*, *Leuconostocaceae*, and *Enterobacteriaceae* are more abundant in 2012 (Fig. 4). Based on associations revealed in the Chardonnay PLSR model (Fig. 3), these alterations relate to the substantially greater net precipitation, RH, and maximum temperatures in 2010 (711.15 cm; 77.6%; 41.1 °C) compared with 2012 (626.31 cm; 74.3%; 36.7 °C).

Bacterial and fungal communities exhibit different responses to vintage and site-specific effects. Vintage and macroregion appear to be the main drivers of bacterial community assembly, and the four individual Napa Chardonnay vineyards are phylogenetically similar (R_{ANOSIM} = 0.024, P = 0.403), even within a single vintage (R_{ANOSIM} = 0.142, P = 0.188) (Table 1), although CDA enables significant (P < 0.0001) discrimination of individual vineyard sites based on the abundance of individual taxa (Fig. 4). Fungal communities within individual vineyards see weak influence from vintage effects and are significantly discriminant across both vintages (R_{ANOSIM} = 0.469, P < 0.001) and within individual vintages (R_{ANOSIM} = 0.442, P < 0.001). CDA also significantly discriminates these vineyards both across and within vintages (P < 0.0001) based on the fungal taxa dominating individual vineyards (Fig. 4). Thus, on site-specific

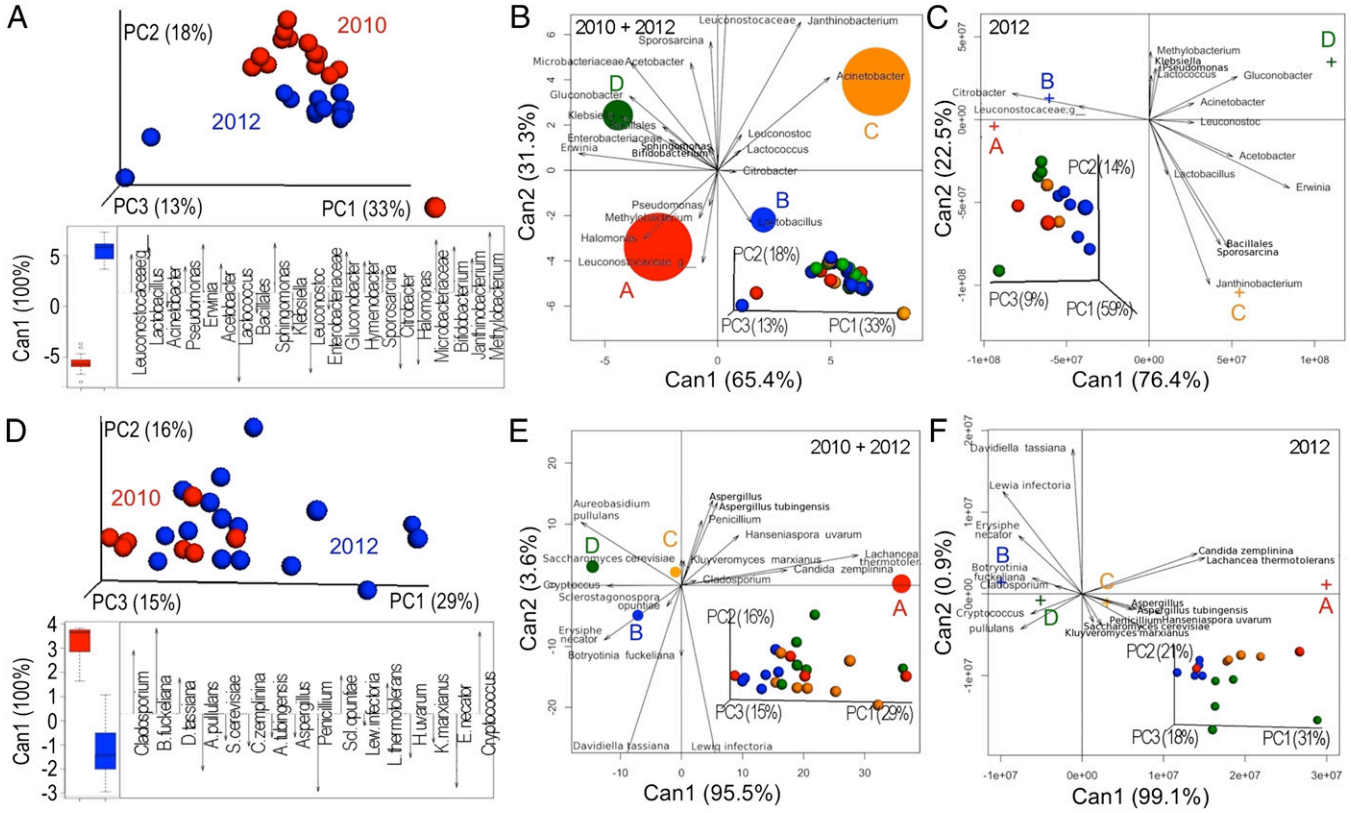

Fig. 4. Vintage affects vineyard-specific microbial patterns. Bacterial (*Upper*) and fungal (*Lower*) communities of Chardonnay musts from four Napa vineyards across 2 y. (*A*) Bacterial weighted UniFrac PCoA (*Upper*) and canonical discriminant analysis (*Lower*) comparing 2010 and 2012 vintages across all vineyards reveal strong vintage effects. (*B* and *C*) CDA plots comparing bacterial communities in musts from four separate vineyards in both vintages (*B*) and in 2012 only (*C*). (*Insets*) Weighted UniFrac PCoA comparison of the complete must bacterial communities in the corresponding vintage(s). (*D*) Fungal Bray–Curtis PCoA (*Upper*) and canonical discriminant analysis (*Lower*) comparing 2010 and 2012 vintages across all vineyards reveal strong vintage effects. (*E* and *F*) CDA plots comparing fungal communities in musts from four separate vineyards in both vintages (*E*) and in 2012 only (*F*). (*Insets*) Bray–Curtis PCoA comparison of the complete must fungal communities in the corresponding vintage(s). CDA circles represent canonical group means and 95% confidence interval for each class, which are significantly different if their confidence intervals do not overlap. Arrows represent the degree of correlation between each taxon and each class as a measure of predictive discrimination of each class.

scales, fungal communities appear more stable than bacterial communities in response to annual climate changes.

The impact of vintage on grape must microbiota fits with the apparent influence of climate and extends these observations. The microbial changes observed between vintages follow the predictions made by the PLSR model, valorizing the potential use of such models for predictions across wider geographical and climatic ranges, provided with appropriately expansive training data. Interestingly, regional and varietal patterns are only weakly influenced by vintage and the strongest effect appears to be (dramatically) observed at the individual vineyard level. This probably reflects the fact that macroregional climate patterns still display greater dissimilarities than local weather variations, where microregional idiosyncrasies may have a tremendous impact, but may also suggest that establishment of regional microbial *terroir* identity resists such ephemeral events. The latter is supported more strongly in the fungal communities, which appear more resistant to vintage variation even with individual vineyards. More annual observations are necessary to determine whether climate induces gradual shifts in regional identity or localized phenomena only.

The discrimination of individual vineyards both within and between vintages reveals important implications for microbial dispersion across small geospatial scales. Setati et al. (52) have demonstrated that intravineyard variation can be greater than intervineyard variation within a single vintage, presumably due to microclimate influences on grape-surface microbiota. By collecting must samples, we have avoided errors arising from such intravineyard variation and sampling biases (i.e., potential spatial variation due to vine position, exposure, microclimate, and stochastic effects), and show that individual vineyard blocks have highly similar must fungal community structures, distinguishing them from neighboring vineyards. As many of the discriminant taxa appear to be fermentative yeasts (Fig. 4), there is a possibility that such intervineyard microbiological variation may help explain the variability frequently witnessed in fermentative performance and product outcomes between different vineyards. Intravineyard block variation may result in further variation observed between different harvest lots, although insufficient block sample replicates were analyzed to test this hypothesis here. Determining how microclimate heterogeneity influences microbial assemblages on the scale of individual vineyards, individual blocks, and individual vines will elucidate how grape-surface microbial communities are established and maintained in response to environmental conditions.

Conclusions

These results represent evidence that grape-associated microbial biogeography is nonrandomly associated with regional, varietal, and climatic factors across multiscale viticultural zones. As the most dominant and discriminant taxa between regions and varieties have well-characterized impacts on grape and wine qual-

ities, these differences may help explain regional patterns in wine chemicosensory properties (29–33). Whether these regionally differential microbiota actually modulate wine sensory qualities must be experimentally tested, as do all putative features of wine *terroir*. This prospective study also reveals several promising applications for grapevine and wine-fermentation management, with the opportunity to develop tailored strategies for improving grape and wine quality of individual varieties and predictive models for microbial community responses to climatic conditions. These exploratory findings pose a paradigm shift in our understanding of food and agricultural systems beyond grape and wine production, wherein microbial communities play active roles in product quality characteristics. Elaboration of the interplay between production region, climate, microbial patterns, and quality outcomes may enhance biological control within these systems, improving the supply, consumer acceptance, and economic value of important agricultural commodities.

Materials and Methods

Data Availability. Raw data are publicly deposited in QIIME-db (microbio.me/qiime/) as studies 2019 (bacterial 16S rRNA sequences) and 2020 (fungal ITS sequences).

Sampling and DNA Extraction. To obtain samples that represent both well-mixed, representative vineyard communities and the microbial consortia introduced into early wine fermentations, grape must was chosen as the optimum sampling point. Grape must consists of destemmed, crushed grapes, which are subsequently pressed (in the case of white wine) and inoculated with *S. cerevisiae* or *Saccharomyces bayanus* to commence fermentation. We chose this as the optimal sampling time, as it represents the junction between grape surface and fermentation microbiota, when all grape-derived microbial inputs are present but inoculation and the onset of fermentation has not yet altered this community.

Grape must samples (n = 235) were collected in 2010 from eight wineries, representing four of the major grape growing regions of California (*SI Appendix*, Fig. S1 and Datasets S9 and S10). In 2012, 39 additional samples were collected from Napa only to test the impact of vintage on microbial patterns within a single growing region. Samples were frozen immediately, shipped on ice, and stored at −80 °C until processing. Sample processing was performed as described previously (14). Briefly, must samples were thawed and centrifuged at 4,000 × g for 15 min, washed three times in ice-cold PBS, suspended in 200 μL DNeasy lysis buffer [20 mM Tris Cl (pH 8.0), 2 mM sodium EDTA, 1.2% Triton X-100] supplemented with 40 mg/mL lysozyme, and incubated at 37 °C for 30 min. From this point, the extraction proceeded following the protocol of the Qiagen Fecal DNA Extraction kit protocol (Qiagen), with the addition of a bead beater cell lysis step of 2 min at maximum speed using a FastPrep-24 bead beater (MP Bio). DNA extracts were stored at −20 °C until further analysis.

Sequencing Library Construction. Amplification and sequencing were performed as described previously for analysis of bacterial (26) and fungal communities (53). Briefly, the V4 domain of bacterial 16S rRNA genes was amplified using primers F515 (5′–*NNNNNNNN***GT**GTGCCAGCMGCCGCGGTAA–3′) and R806 (5′–GGACTACHVGGGTWTCTAAT–3′) (54), with the forward primer modified to contain a unique 8-nt barcode (italicized poly-N section of primer above) and a 2-nt linker sequence (bold portion) at the 5′ terminus. All F515 primer barcodes used are presented in Dataset S9. PCR reactions contained 5–100 ng DNA template, 1× GoTaq Green Master Mix (Promega), 1 mM MgCl2, and 2 pmol of each primer. Reaction conditions consisted of an initial 94 °C for 3 min followed by 35 cycles of 94 °C for 45 s, 50 °C for 60 s, and 72 °C for 90 s, and a final extension of 72 °C for 10 min. Fungal internal transcribed spacer (ITS) 1 loci were amplified with primers BITS (5′–*NNNNNNNN***CT**ACCTGCGGARGGATCA–3′) and B58S3 (5′–GAGATCCRTTGYTRAAAGTT–3′) (53), with a unique 8-nt barcode and linker sequence (bold portion) incorporated in each forward primer. All BITS primer barcodes used are presented in Dataset S10. PCR reactions contained 5–100 ng DNA template, 1× GoTaq Green Master Mix (Promega), 1 mM MgCl2, and 2 pmol of each primer. Reaction conditions consisted of an initial 95 °C for 2 min followed by 40 cycles of 95 °C for 30 s, 55 °C for 30 s, and 72 °C for 60 s, and a final extension of 72 °C for 5 min. Amplicons were combined into two separate pooled samples (keeping bacterial and fungal amplicons separate) at roughly equal amplification intensity ratios, purified using the Qiaquick spin kit (Qiagen), and submitted to the University of California Davis Genome Center DNA Technologies Core for Illumina paired-end library preparation, cluster generation, and 250-bp paired-end sequencing on an Illumina MiSeq instrument in two separate runs. Following quality filtering (see below), the first (bacterial 16S rRNA) run generated 5,120,803 reads (247.35 nt mean length) and the second (fungal ITS) run generated 3,241,736 reads (245.43 nt mean length). Sequence rarefaction curves, demonstrating per-sample sequence coverage, are shown in *SI Appendix*, Fig. S10.

Data Analysis. Raw Illumina fastq files were demultiplexed, quality filtered, and analyzed using QIIME v1.7.0 (55). Reads were truncated at any site containing more than three consecutive bases receiving a quality score <1e-5, and any read containing one or more ambiguous base calls was discarded, as were truncated reads of <190 nt. Operational taxonomic units (OTUs) were assigned using QIIME's uclust-based (56) open-reference OTU-picking workflow, with a threshold of 97% pairwise identity. Sequence prefiltering (discarding sequences with <60% pairwise identity to any reference sequence) and reference-based OTU picking were performed using a representative subset of the Greengenes bacterial 16S rRNA database (13_5 release) (57) or the UNITE fungal ITS database (12_9 release) (58), filtered to remove incomplete and unannotated taxonomies (53). OTUs were classified taxonomically using a QIIME-based wrapper of the Ribosomal Database Project (RDP) classifier (59) against a representative subset of the Greengenes 16S rRNA database 13_5 release (57), using a 0.50 confidence threshold for taxonomic assignment. Bacterial 16S rRNA gene sequences were aligned using PyNAST (60) against a template alignment of the Greengenes core set filtered at 97% similarity. From this alignment, chimeric sequences were identified and removed using ChimeraSlayer (61) and a phylogenic tree was generated from the filtered alignment using FastTree (62). Sequences failing alignment or identified as chimeric were removed before downstream analysis. Any OTU representing less than 0.001% of the total filtered sequences was removed to avoid inclusion of erroneous reads, leading to inflated estimates of diversity (63), as were samples represented by less than 200 (bacterial) or 1,000 (fungal) sequences following all quality-filtering steps.

Alpha-diversity (within-sample species richness) and beta-diversity (between-sample community dissimilarity) estimates were calculated within QIIME using weighted UniFrac (28) distance between samples for bacterial 16S rRNA reads [evenly sampled at 1,000 (for Chardonnay-only analysis) or 200 reads per sample] and Bray–Curtis dissimilarity for fungal ITS reads (evenly sampled at 1,000 reads per sample). Principal coordinates were computed from the resulting distance matrices to compress dimensionality intro 3D principal coordinate analysis (PCoA) plots, enabling visualization of sample relationships. To determine whether sample classifications (region, variety, vineyard, vintage) contained differences in phylogenetic or species diversity, ANOSIM (64) and permutational MANOVA (65) with 999 permutations were used to test significant differences between sample groups based on weighted UniFrac (28) and Bray–Curtis distance matrices. For all categorical classifications (region, vintage, variety, vineyard) rejecting this null hypothesis, one-way ANOVA was used to determine which taxa differed between sample groups, resulting in these differences. A BEST was used to rank the importance of environmental features in influencing beta-diversity community comparisons, with feature significance confirmed with permutational MANOVA.

Random forest supervised-classification models (66) were used to identify taxonomic features that explain the strongest variation between sample conditions and evaluate the diagnostic strength of these features to discriminate against regional categories. Ten-fold cross-validation models were constructed with 1,000 trees, using taxonomic assignments of evenly rarefied sample OTUs as predictors and regional origin as class labels.

Significant taxonomic differences between sample conditions were also tested using LDA effect size (67). This method employs the factorial Kruskal–Wallis sum-rank test (α = 0.05) to identify taxa with significant differential abundances between categories (using one-against-all comparisons), followed by LDA to estimate the effect size of each differentially abundant feature. Significant taxa were used to generate taxonomic cladograms illustrating differences between sample classes.

Geospatial biodiversity mapping analysis was performed using GenGIS II (68). This method was used to determine significant fitness between geographical coordinates along linear axes and sample ordination on phylogenetic (bacterial 16S rRNA weighted UniFrac) (28) or taxonomic dissimilarity (fungal ITS Bray–Curtis) unweighted pair group method with arithmetic mean (UPGMA) trees constructed in QIIME.

All other statistical tests were performed in R software (v 2.15.0). CDA was used to describe differences between sample categories and identify taxa associated with each condition. PLSR analysis with cross-validation was used to model associations between normalized mean values for significant

environmental conditions (*X* variables) and taxonomic features (*Y* variables). Pearson product–moment correlation coefficients, Spearman rank correlation coefficients, and scatterplots were used to test and visualize relationships between topographical and climatic features.

Climate Data. Daily weather data were extracted from the California Irrigation Management Information System (CIMIS) database (www.cimis.water.ca.gov/). Data were collected from 19 different weather stations throughout California representing the nearest CIMIS station to each source vineyard. Daily measurements were extracted for average high temperature, average low temperature, average temperature, maximum temperature, minimum temperature, net precipitation, average ET_0, average solar radiation, average soil temperature, average wind speed, net wind run, and average RH in 2010 and 2012 for all stations.

ACKNOWLEDGMENTS. The authors thank Rob Knight and Greg Caporaso for critical review of the manuscript; Mariya Ryazantseva for technical assistance with molecular methods; Mariko Zelin and Chad Masarweh for assistance with DNA extractions; and Greg Gessner, Steve Smit, Jim Orvis, Oren Kaye, Jan Kappmeyer, and Chris Cunningham (Constellation Brands, Inc.) for their contributions and in-kind support toward sample and metadata collection. N.A.B. was supported by the American Wine Society Educational Foundation Endowment Fund Scholarship, the Brian Williams Scholarship (American Society of Brewing Chemists Foundation), Wine Spectator, and Grant T32-GM008799 from National Institute of General Medical Sciences–National Institutes of Health during the completion of this work.

1. Martiny JB, et al. (2006) Microbial biogeography: Putting microorganisms on the map. *Nat Rev Microbiol* 4(2):102–112.
2. Koren O, et al. (2012) Host remodeling of the gut microbiome and metabolic changes during pregnancy. *Cell* 150(3):470–480.
3. Gibbons SM, et al. (2013) Evidence for a persistent microbial seed bank throughout the global ocean. *Proc Natl Acad Sci USA* 110(12):4651–4655.
4. Adams RI, Miletto M, Taylor JW, Bruns TD (2013) Dispersal in microbes: Fungi in indoor air are dominated by outdoor air and show dispersal limitation at short distances. *ISME J* 7(7):1262–1273.
5. Peiffer JA, et al. (2013) Diversity and heritability of the maize rhizosphere microbiome under field conditions. *Proc Natl Acad Sci USA* 110(16):6548–6553.
6. Barata A, Malfeito-Ferreira M, Loureiro V (2012) The microbial ecology of wine grape berries. *Int J Food Microbiol* 153(3):243–259.
7. Lonvaud-Funel A (1999) Lactic acid bacteria in the quality improvement and depreciation of wine. *Antonie van Leeuwenhoek* 76(1-4):317–331.
8. Swiegers JH, Bartowsky E, Henschke PA, Pretorius IS (2005) Yeast and bacterial modulation of wine aroma and flavour. *Aust J Grape Wine Res* 11(2):139–173.
9. Van Leeuwen C, Seguin G (2006) The concept of terroir in viticulture. *J Wine Res* 17(1): 1–10.
10. Renouf V, Claisse O, Lonvaud-Funel A (2007) Inventory and monitoring of wine microbial consortia. *Appl Microbiol Biotechnol* 75(1):149–164.
11. Jackson DI, Lombard PB (1993) Environmental and management practices affecting grape composition and wine quality—a review. *Am J Enol Vitic* 44(4):409–430.
12. Hong Y-S, et al. (2011) Metabolic influence of *Botrytis cinerea* infection in champagne base wine. *J Agric Food Chem* 59(13):7237–7245.
13. Tosi E, et al. (2013) Induction of grape botrytization during withing affects volatile composition of Recioto di Soave, a "passito"-style wine. *Eur Food Res Technol* 236: 853–862.
14. Bokulich NA, Joseph CML, Allen GR, Benson A, Mills DA (2012) Next-generation sequencing reveals significant bacterial diversity of botrytized wine. *PLoS ONE* 7(5): e36357.
15. Barata A, González S, Malfeito-Ferreira M, Querol A, Loureiro V (2008) Sour rot-damaged grapes are sources of wine spoilage yeasts. *FEMS Yeast Res* 8(7):1008–1017.
16. Joyeux A, Lafon-Lafourcade S, Ribéreau-Gayon P (1984) Evolution of acetic acid bacteria during fermentation and storage of wine. *Appl Environ Microbiol* 48(1): 153–156.
17. Ciani M, Comitini F, Mannazzu I, Domizio P (2010) Controlled mixed culture fermentation: A new perspective on the use of non-Saccharomyces yeasts in winemaking. *FEMS Yeast Res* 10(2):123–133.
18. Gayevskiy V, Goddard MR (2012) Geographic delineations of yeast communities and populations associated with vines and wines in New Zealand. *ISME J* 6(7):1281–1290.
19. Bokulich NA, Mills DA Next-generation approaches to the microbial ecology of food fermentations*BMB Rep*(2012) 457377–389.
20. Bokulich NA, Bamforth CW, Mills DA (2012) A review of molecular methods for microbial community profiling of beer and wine. *J. Am. Soc. Brew. Chem.* 70:150–162.
21. Humblot C, Guyot J-P (2009) Pyrosequencing of tagged 16S rRNA gene amplicons for rapid deciphering of the microbiomes of fermented foods such as pearl millet slurries. *Appl Environ Microbiol* 75(13):4354–4361.
22. Roh SW, et al. (2010) Investigation of archaeal and bacterial diversity in fermented seafood using barcoded pyrosequencing. *ISME J* 4(1):1–16.
23. Alegría A, Szczesny P, Mayo B, Bardowski J, Kowalczyk M (2012) Biodiversity in Oscypek, a traditional Polish cheese, determined by culture-dependent and -independent approaches. *Appl Environ Microbiol* 78(6):1890–1898.
24. Bokulich NA, Bamforth CW, Mills DA (2012) Brewhouse-resident microbiota are responsible for multi-stage fermentation of American coolship ale. *PLoS ONE* 7(4): e35507.
25. Bokulich NA, Mills DA (2013) Facility-specific "house" microbiome drives microbial landscapes of artisan cheesemaking plants. *Appl Environ Microbiol* 79(17):5214–5223.
26. Bokulich NA, Ohta M, Richardson PM, Mills DA (2013) Monitoring seasonal changes in winery-resident microbiota. *PLoS ONE* 8(6):e66437.
27. De Filippis F, La Storia A, Villani F, Ercolini D (2013) Exploring the sources of bacterial spoilers in beefsteaks by culture-independent high-throughput sequencing. *PLoS ONE* 8(7):e70222.
28. Lozupone CA, Knight R (2005) UniFrac: A new phylogenetic method for comparing microbial communities. *Appl Environ Microbiol* 71(12):8228–8235.
29. Pereira GE, et al. (2005) 1H NMR and chemometrics to characterize mature grape berries in four wine-growing areas in Bordeaux, France. *J Agric Food Chem* 53(16):6382–6389.
30. Son HS, et al. (2009) Metabolomic studies on geographical grapes and their wines using 1H NMR analysis coupled with multivariate statistics. *J Agric Food Chem* 57(4):1481–1490.
31. López-Rituerto E, et al. (2012) Investigations of La Rioja terroir for wine production using ^{1}H NMR metabolomics. *J Agric Food Chem* 60(13):3452–3461.
32. Fischer U, Roth D, Christmann M (1999) The impact of geographic origin, vintage, and wine estate on sensory properties of *Vitis vinifera* cv. Riesling wines. *Food Qual Prefer* 10:281–288.
33. Robinson AL, et al. (2012) Influence of geographic origin on the sensory characteristics and wine composition of *Vitis vinifera* cv. Cabernet sauvignon wines from Australia. *Am J Enol Vitic* 63(4):467–476.
34. Fleet GH (2008) Wine yeasts for the future. *FEMS Yeast Res* 8(7):979–995.
35. Sabate J, Cano J, Esteve-Zarzoso B, Guillamón JM (2002) Isolation and identification of yeasts associated with vineyard and winery by RFLP analysis of ribosomal genes and mitochondrial DNA. *Microbiol Res* 157(4):267–274.
36. Cordero-Bueso G, et al. (2011) Influence of the farming system and vine variety on yeast communities associated with grape berries. *Int J Food Microbiol* 145(1):132–139.
37. Renouf V, Claisse O, Lonvaud-Funel A (2005) Understanding the microbial ecosystemon the grape berry surface through numeration and identification of yeast and bacteria. *Aust J Grape Wine Res* 11:316–327.
38. Fung RW, et al. (2008) Powdery mildew induces defense-oriented reprogramming of the transcriptome in a susceptible but not in a resistant grapevine. *Plant Physiol* 146(1):236–249.
39. Smith RJ (2003) Zinfandel. *Wine Grape Varieties in California*, ed Christensen LP (University of California Agriculture and Natural Resources, Oakland, CA).
40. Barata A, Malfeito-Ferreira M, Loureiro V (2012) Changes in sour rotten grape berry microbiota during ripening and wine fermentation. *Int J Food Microbiol* 154(3):152–161.
41. Pereira GE, et al. (2006) Microclimate influence on mineral and metabolic profiles of grape berries. *J Agric Food Chem* 54(18):6765–6775.
42. Holt HE, Francis IL, Field J, Herderich MJ, Iland PG (2008) Relationships between berry size, berry phenolic composition and wine quality scores for Cabernet Sauvignon (Vitis viniferaL.) from different pruning treatments and different vintages. *Aust J Grape Wine Res* 14(3):191–202.
43. Tofalo R, et al. (2012) Diversity of Candida zemplinina strains from grapes and Italian wines. *Food Microbiol* 29(1):18–26.
44. Austin CN, Grove GG, Meyers JM, Wilcox WF (2011) Powdery mildew severity as a function of canopy density: Associated impacts on sunlight penetration and spray coverage. *Am J Enol Vitic* 62(1):23–31.
45. Hannah L, et al. (2013) Climate change, wine, and conservation. *Proc Natl Acad Sci USA* 110(17):6907–6912.
46. Burie JB, Langlais M, Calonnec A (2011) Switching from a mechanistic model to a continuous model to study at different scales the effect of vine growth on the dynamic of a powdery mildew epidemic. *Ann Bot (Lond)* 107(5):885–895.
47. Pugliese M, Gullino ML, Garibaldi A Effect of climate change on infection of grapevine by downy and powdery mildew under controlled environment*Commun Agric Appl Biol Sci*(2011) 764579–582.
48. Weber E, Gubler D, Derr A Powdery mildew controlled with fewer fungicide applications. Practical Winery & Vineyard (January/February).
49. Pfender WF, Gent DH, Mahaffee WF, Coop LB, Fox AD (2011) Decision aids for multiple-decision disease management as affected by weather input errors. *Phytopathology* 101(6):644–653.
50. Fernández-González M, et al. (2012) Forecasting ARIMA models for atmospheric vineyard pathogens in Galicia and Northern Portugal: *Botrytis cinerea* spores. *Ann Agric Environ Med* 19(2):255–262.
51. Larsen PE, Field D, Gilbert JA (2012) Predicting bacterial community assemblages using an artificial neural network approach. *Nat Methods* 9(6):621–625.
52. Setati ME, Jacobson D, Andong UC, Bauer F (2012) The vineyard yeast microbiome, a mixed model microbial map. *PLoS ONE* 7(12):e52609.
53. Bokulich NA, Mills DA (2013) Improved selection of internal transcribed spacer-specific primers enables quantitative, ultra-high-throughput profiling of fungal communities. *Appl Environ Microbiol* 79(8):2519–2526.
54. Caporaso JG, et al. (2011) Global patterns of 16S rRNA diversity at a depth of millions of sequences per sample. *Proc Natl Acad Sci USA* 108(Suppl 1):4516–4522.
55. Caporaso JG, et al. (2010) QIIME allows analysis of high-throughput community sequencing data. *Nat Methods* 7(5):335–336.
56. Edgar RC (2010) Search and clustering orders of magnitude faster than BLAST. *Bioinformatics* 26(19):2460–2461.
57. DeSantis TZ, et al. (2006) Greengenes, a chimera-checked 16S rRNA gene database and workbench compatible with ARB. *Appl Environ Microbiol* 72(7):5069–5072.

58. Abarenkov K, et al. (2010) The UNITE database for molecular identification of fungi—recent updates and future perspectives. *New Phytol* 186(2):281–285.
59. Wang Q, Garrity GM, Tiedje JM, Cole JR (2007) Naive Bayesian classifier for rapid assignment of rRNA sequences into the new bacterial taxonomy. *Appl Environ Microbiol* 73(16):5261–5267.
60. Caporaso JG, et al. (2010) PyNAST: A flexible tool for aligning sequences to a template alignment. *Bioinformatics* 26(2):266–267.
61. Haas BJ, et al.; Human Microbiome Consortium (2011) Chimeric 16S rRNA sequence formation and detection in Sanger and 454-pyrosequenced PCR amplicons. *Genome Res* 21(3):494–504.
62. Price MN, Dehal PS, Arkin AP (2010) FastTree 2—approximately maximum-likelihood trees for large alignments. *PLoS ONE* 5(3):e9490.
63. Bokulich NA, et al. (2013) Quality-filtering vastly improves diversity estimates from Illumina amplicon sequencing. *Nat Methods* 10(1):57–59.
64. Clarke KR (1993) Non-parametric multivariate analysis of changes in community structure. *Aust J Ecol* 18:117–143.
65. Anderson MJ (2001) A new method for non-parametric multivariate analysis of variance. *Austral Ecol* 26:32–46.
66. Liaw A, Weiner M (2002) Classification and regression by RandomForest. *R News* 2(3):18–22.
67. Segata N, et al. (2011) Metagenomic biomarker discovery and explanation. *Genome Biol* 12(6):R60.
68. Parks DH, et al. (2013) GenGIS 2: Geospatial analysis of traditional and genetic biodiversity, with new gradient algorithms and an extensible plugin framework. *PLoS ONE* 8(7):e69885.